

Exploiting Starlink Signals for Navigation: First Results

Mohammad Neinavaie, Joe Khalife, and Zaher M. Kassas
University of California, Irvine

BIOGRAPHIES

Mohammad Neinavaie is a Ph.D. student at the University of California, Irvine and member of the Autonomous Systems Perception, Intelligence, and Navigation (ASPIN) Laboratory. He received a B.E. in electrical engineering and an M.S. in digital communication systems from Shiraz University. His research interests include opportunistic navigation, blind opportunistic navigation, cognitive radio, wireless communication systems and software-defined radio.

Joe J. Khalife is a postdoctoral fellow at the University of California, Irvine and member of the Autonomous Systems Perception, Intelligence, and Navigation (ASPIN) Laboratory. He received a B.E. in electrical engineering, an M.S. in computer engineering from the Lebanese American University (LAU) and a Ph.D. in electrical engineering from the University of California, Irvine. From 2012 to 2015, he was a research assistant at LAU. His research interests include opportunistic navigation, autonomous vehicles, and software-defined radio.

Zaher (Zak) M. Kassas is an associate professor at the University of California, Irvine and director of the Autonomous Systems Perception, Intelligence, and Navigation (ASPIN) Laboratory. He is also director of the U.S. Department of Transportation Center: CARMEN (Center for Automated Vehicle Research with Multimodal AssurEd Navigation), focusing on navigation resiliency and security of highly automated transportation systems. He received a B.E. in Electrical Engineering from the Lebanese American University, an M.S. in Electrical and Computer Engineering from The Ohio State University, and an M.S.E. in Aerospace Engineering and a Ph.D. in Electrical and Computer Engineering from The University of Texas at Austin. He is a recipient of the 2018 National Science Foundation (NSF) Faculty Early Career Development Program (CAREER) award, 2019 Office of Naval Research (ONR) Young Investigator Program (YIP) award, 2018 IEEE Walter Fried Award, 2018 Institute of Navigation (ION) Samuel Burka Award, and 2019 ION Col. Thomas Thurlow Award. His research interests include cyber-physical systems, estimation theory, navigation systems, autonomous vehicles, and intelligent transportation systems.

ABSTRACT

This paper demonstrates the first Doppler positioning-based results with Starlink low Earth orbit (LEO) satellites. A cognitive opportunistic framework is used to detect Starlink's LEO satellite signals and track the Doppler frequencies of each Starlink LEO satellite. To this end, a generalized likelihood ratio (GLR)-based test is developed to detect the LEO satellite signals and estimate their corresponding beacons. A chirp parameter estimator is also proposed to track the Doppler frequencies from the unknown Starlink signals. Experimental results are presented showing a horizontal positioning error of 10 m by tracking the Doppler of six Starlink LEO satellites.

I. INTRODUCTION

Theoretical and experimental studies demonstrated the potential of low Earth orbit (LEO) broadband communication satellites as promising reliable sources for navigation [1–14]. Companies like Amazon, Telesat, OneWeb, and SpaceX are deploying so-called *megaconstellations* to provide global broadband internet [15, 16]. In particular, launching thousands of space vehicles (SVs) into LEO by SpaceX, can be considered as a turning-point in the future of LEO-based navigation technologies. Signals received by LEO SVs can be about 30 dB stronger than signals received from medium Earth orbit (MEO) where global navigation satellite systems (GNSS) SVs are placed [17].

Research has shown that one could exploit LEO SV broadband communication signals opportunistically for navigation purposes [18, 19]. Opportunistic navigation exempts the broadband provider from radical system changes, and does not require additional costly services and infrastructures. However, in order to draw navigation observables, an opportunistic framework needs knowledge of the LEO SV signal structure which may not be publicly available. Three of the main challenges of navigation with Starlink SV signals are (i) limited information about the signal structure, (ii) very-high

dynamics of Starlink LEO SVs, and (iii) unknown ephemerides. This paper mainly concentrates on the first and second challenges.

The detection problem of an unknown source in the presence of other interfering signals falls into the paradigm of *matched subspace detectors* which has been widely studied in the classic detection literature [20–22]. Matched subspace detectors are used frequently in radar signal processing, e.g., in source localization in multiple-input multiple-output (MIMO) radars [23] and passive bistatic radar [24]. In [25], the design of subspace matched filters in the presence of mismatch in the steering vector was addressed. The performance of low-rank adaptive normalized matched subspace detectors was studied in [26]. In [27], the idea of subspace matching was used to present a solution to the problem of detecting the number of signals in both white and colored noise. In [28], the structure of the noise covariance matrix was exploited to enhance the matched subspace detection performance. In [29], adaptive vector subspace detection in partially homogeneous Gaussian disturbance was addressed. In the navigation literature, detection of unknown signals has been studied to design frameworks which are capable of navigating with unknown or partially known signals. The problem of detecting Galileo and Compass SV signals was studied in [30], which revealed the spread spectrum codes for these SVs. Preliminary experiments on navigation with partially known signals from low and medium Earth orbit satellites were conducted in [31–33]. In [34], a cognitive opportunistic navigation framework was proposed to exploit 5G signals for navigation purposes. This paper builds on the concept of cognitive opportunistic navigation by presenting a receiver architecture, which is capable of exploiting Starlink signals for navigation. Assuming that Starlink LEO SV downlink signals contains a periodic reference signal (RS), this paper formulates a *matched subspace detection* problem to detect the unknown RSs of Starlink SVs and estimating the unknown period and Doppler frequency.

This paper makes the following contributions. First, a model for the Starlink LEO SV’s downlink signals is presented. Second, an algorithm is proposed to (i) acquire the Starlink LEO SV signals and (ii) track the Doppler frequency of each detected SV. Third, next to [19], the first experimental results with Starlink downlink signals is presented in this paper. In [19], a phase-locked loop was used to track the carrier phase of Starlink LEO SVs. However, the method presented in [19] relies on tracking the phase of a single carrier at a time, but does not generalize to more complicated structures, e.g., orthogonal frequency-division multiple access (OFDMA). In this paper, by considering a general model for the Starlink downlink signals, the unknown parameters of the signal are estimated and used to detect Starlink LEO SVs. Indeed, the proposed method enables one to estimate the synchronization signals of the Starlink LEO SVs. A demonstration of the first Starlink LEO SVs detection, Doppler tracking, and positioning results with real Starlink signals is presented, showing a horizontal position error of 10 m with six Starlink SVs.

The rest of the paper is organized as follows. Section II presents the hardware setup. Section III describes the received baseband signal model. Section IV and V present the proposed acquisition and Doppler tracking methods, respectively. Section VI presents the experimental results. Section VII gives concluding remarks.

II. DOWNCONVERTING STARLINK LEO SV SIGNALS

Detailed signal specifications of Starlink downlink signals are not available to the public. The only known information about these signals are the carrier frequencies and the bandwidths. The Ku-band is used by SpaceX for the satellite-to-user links (both uplink and downlink) [35]. In order to sample bands of the radio frequency, software-defined radios (SDRs) can be used. However, Ku/Ka bands are beyond the carrier frequency of most commercial SDRs.

In this paper, a hardware setup is proposed based on downconverting the Starlink LEO SV signals to the L band. A 10 GHz mixer is employed between the antenna and the SDR to downconvert Starlink LEO SV signals from the Ku band (10.7–12.75 GHz) to the L band (950–2150 MHz). In particular, the hardware downconverts the Starlink LEO SV Ku band signals, namely 11.325 GHz, to 1.325 GHz. The hardware block diagram can be seen in Fig. 1.

In order to formulate a detection problem to detect the activity of Starlink downlink signals, a signal model is proposed which solely relies on the periodicity of the transmitted signals. The logic behind the proposed signal model is that in most commercial communication systems, a periodic RS is transmitted for synchronization purposes, e.g., primary synchronization signals (PSS) in long term evolution (LTE) and the fifth generation (5G) signals [36]. The following subsection, presents a model for the Starlink LEO SV’s downlink signals. Moreover, in order to capture the high dynamics of the Starlink LEO SVs, the proposed signal model considers a *second-order polynomial* model for the variations of the Doppler frequency in the processing interval.

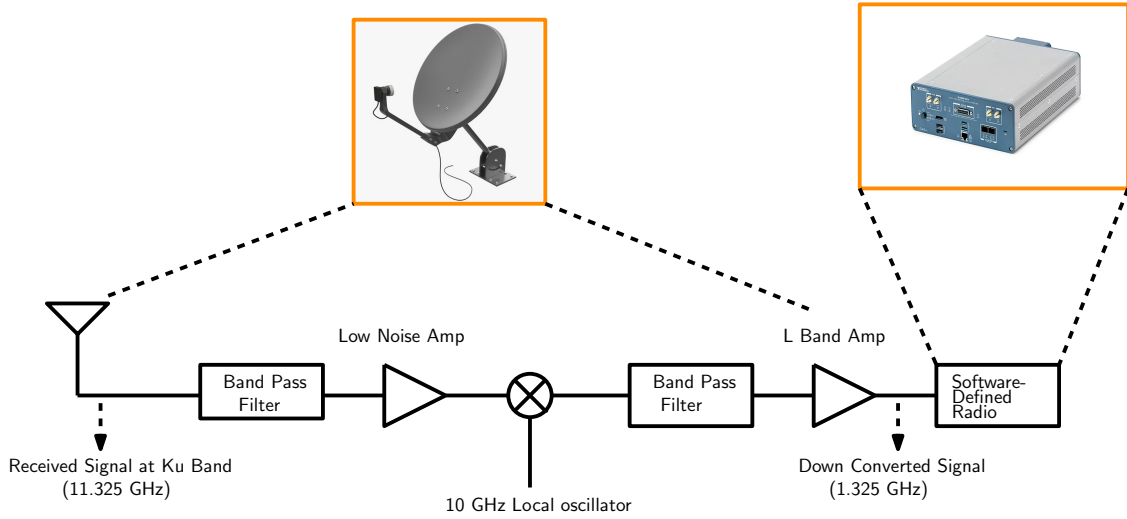


Fig. 1. Two stages down-converter.

III. PROPOSED SIGNAL MODEL FOR STARLINK LEO SV DOWNLINK SIGNALS

As it was mentioned previously, in most commercial communication systems, a periodic RS is transmitted, e.g., PSS in OFDMA-based and spreading codes in code division multiple access (CDMA)-based signals [37]. In this paper, the Starlink LEO SV downlink signal is modeled as an unknown periodic signal in the presence of interference and noise. If an RS such as PSS in OFDMA-based signals is being periodically transmitted, it will be detected and estimated by the proposed method. The proposed signal model is

$$r[n] = \alpha c[\tau_n - t_s[n]] \exp(j\theta[\tau_n]) + d[\tau_n - t_s[n]] \exp(j\theta[\tau_n]) + w[n], \quad (1)$$

where $r[n]$ is the received signal at the n th time instant; α is the complex channel gain between the receiver and the Starlink LEO SV; τ_n is the sample time expressed in the receiver time; $c[\tau_n]$ represents the samples of the complex periodic RS with a period of L samples; $t_s[n]$ is the code-delay corresponding to the receiver and the Starlink LEO SV at the n th time instant; $\theta[\tau_n] = 2\pi f_D[n]T_s n$ is the carrier phase in radians, where $f_D[n]$ is the instantaneous Doppler frequency at the n th time instant and T_s is the sampling time; $d_i[\tau_n]$ represents the complex samples of some data transmitted from the Starlink LEO SV; and $w[n]$ is the complex zero-mean independent and identically distributed noise with variance σ_w^2 .

Starlink LEO SV's signals suffer from very high Doppler shifts. Higher lengths of processing intervals require higher order Doppler models. In order for a Doppler estimation algorithm to provide an accurate estimation of the Doppler frequency, the processing interval should be large enough to accumulate enough energy. According to the considered processing interval length in the experiments, it is observed that during the k th processing interval the instantaneous Doppler frequency is almost a linear function of time, i.e., $f_D[n] = f_{D_k} + \beta_k n$, where f_{D_k} is referred to as constant Doppler, and β_k is the Doppler rate at the k th processing interval. The coherent processing interval (CPI) is defined as the time interval in which the constant Doppler, f_{D_k} , and the Doppler rate, β_k , are constant.

The received signal at the n th time instant when the Doppler rate is wiped-off is denoted by $r'[n] \triangleq \exp(-j2\pi\beta_k n^2)r[n]$. One can define the *desired RS* which is going to be detected in the acquisition stage as

$$s[n] \triangleq \alpha c[\tau_n - t_s[n]] \exp(j2\pi f_{D_k} T_s n), \quad (2)$$

and the equivalent noise as

$$w_{\text{eq}}[n] = d[\tau_n - t_s[n]] \exp(j2\pi f_{D_k} T_s n) + \exp(-j2\pi\beta_k n^2) w[n]. \quad (3)$$

Hence, $r'[n] = s[n] + w_{\text{eq}}[n]$. Due to the periodicity of the RS, $s[n]$ has the following property

$$s[n + mL] = s[n] \exp(j\omega_k mL) \quad 0 \leq n \leq L - 1, \quad (4)$$

where $\omega_k = 2\pi f_{D_k} T_s$ is the normalized Doppler at the k th CPI, and $-\frac{1}{2} \leq \omega_k \leq \frac{1}{2}$. A vector of L observation samples corresponding to the m th period of the signal is formed as

$$\mathbf{z}_m \triangleq [r'[mL], r'[mL+1], \dots, r'[(m+1)L-1]]^T. \quad (5)$$

The k th CPI vector is constructed by concatenating M vectors of length L to form the $ML \times 1$ vector

$$\mathbf{y}_k = [\mathbf{z}_{kM}^T, \mathbf{z}_{kM+1}^T, \dots, \mathbf{z}_{(k+1)M-1}^T]^T. \quad (6)$$

Therefore,

$$\mathbf{y}_k = \mathbf{H}_k \mathbf{s} + \mathbf{w}_{\text{eqk}}, \quad (7)$$

where $\mathbf{s} = [s[1], s[2], \dots, s[L]]^T$, and the $ML \times L$ Doppler matrix is defined as

$$\mathbf{H}_k \triangleq [\mathbf{I}_L, \exp(j\omega_k L) \mathbf{I}_L, \dots, \exp(j\omega_k (M-1)L) \mathbf{I}_L]^T, \quad (8)$$

where \mathbf{I}_L is an $L \times L$ identity matrix, and \mathbf{w}_{eqk} is the equivalent noise vector.

IV. ACQUISITION

In this section, a detection scheme is proposed to detect the existence of Starlink LEO SVs in the carrier frequency of 11.325 GHz within a bandwidth of 2.5 MHz, at $k = 0$. The following binary hypothesis test is used to detect the Starlink LEO SV

$$\begin{cases} \mathcal{H}_0 : \mathbf{y}_0 = \mathbf{w}_{\text{eq}_0} \\ \mathcal{H}_1 : \mathbf{y}_0 = \mathbf{H}_0 \mathbf{s} + \mathbf{w}_{\text{eq}_0}. \end{cases} \quad (9)$$

For a given set of unknown variables $\mathcal{W}_0 = \{L, \omega_0, \beta_0\}$, the GLR detector for the testing hypothesis (9) is known as matched subspace detector [20, 22], and is derived as (see Theorem 9.1 in [38])

$$\mathcal{L}(\mathbf{y}_0 | \mathcal{W}_0) = \frac{\mathbf{y}_0^H \mathbf{P}_{\mathbf{H}_0} \mathbf{y}_0}{\mathbf{y}_0^H \mathbf{P}_{\mathbf{H}_0}^\perp \mathbf{y}_0} \underset{\mathcal{H}_0}{\overset{\mathcal{H}_1}{\geq}} \eta, \quad (10)$$

where \mathbf{y}_0^H is the Hermitian transpose of \mathbf{y}_0 , $\mathbf{P}_{\mathbf{H}_0} \triangleq \mathbf{H}_0 (\mathbf{H}_0^H \mathbf{H}_0)^{-1} \mathbf{H}_0^H$ denotes the projection matrix to the column space of \mathbf{H}_0 , $\mathbf{P}_{\mathbf{H}_0}^\perp \triangleq \mathbf{I} - \mathbf{P}_{\mathbf{H}_0}$ denotes the projection matrix onto the space orthogonal to the column space of \mathbf{H}_0 , and η is the threshold which is predetermined according to the probability of false alarm. Since, $\mathbf{H}_k^H \mathbf{H}_k = M \mathbf{I}_L$ for all k , the likelihood can be rewritten as $\mathcal{L}(\mathbf{y}_0 | \mathcal{W}_0) = \frac{1}{\frac{1}{M^2} \frac{\|\mathbf{H}_0^H \mathbf{y}_0\|^2}{\|\mathbf{y}_0\|^2} - 1}$, which is a monotonically increasing function of $\frac{\|\mathbf{H}_0^H \mathbf{y}_0\|^2}{\|\mathbf{y}_0\|^2}$. Hence, the GLR

detector (10) is equivalent to

$$\frac{\|\mathbf{H}_0^H \mathbf{y}_0\|^2}{\|\mathbf{y}_0\|^2} \underset{\mathcal{H}_0}{\overset{\mathcal{H}_1}{\geq}} \eta', \quad (11)$$

where η' is determined according to the desired probability of false alarm. The maximum likelihood of the set \mathcal{W}_0 is

$$\hat{\mathcal{W}}_0 = \underset{L, \omega_0, \beta_0}{\text{argmax}} \|\mathbf{H}_0^H \mathbf{y}_0\|^2, \quad (12)$$

It should be pointed out that the estimated Doppler using (12) results in a constant ambiguity denoted by $\omega_0 = 2\pi f_0$. This constant ambiguity is accounted for in the navigation filter.

Fig. 2 demonstrates the likelihood in terms of Doppler frequency and the period for real Starlink downlink signals. The CPI is considered to be 200 times the period. The Doppler-beacon length subspace for two time instances t_0 and t_1 where $t_1 - t_0 = 1$ s. As it can be seen in this figure, the likelihood's location is changed from t_0 to t_1 in the subspace which demonstrates a Doppler rate of 1609 Hz/s for this Starlink LEO SV.

V. Doppler Tracking

The low effective SNR per *degree of freedom* in many scenarios, e.g., OFDMA-based signals, may impose a large CPI. The Doppler estimator in the proposed receiver processes one CPI at a time to estimate the Doppler parameters corresponding to the CPI. To accumulate enough energy, the number of samples in one CPI, i.e., M , has to be large enough to include

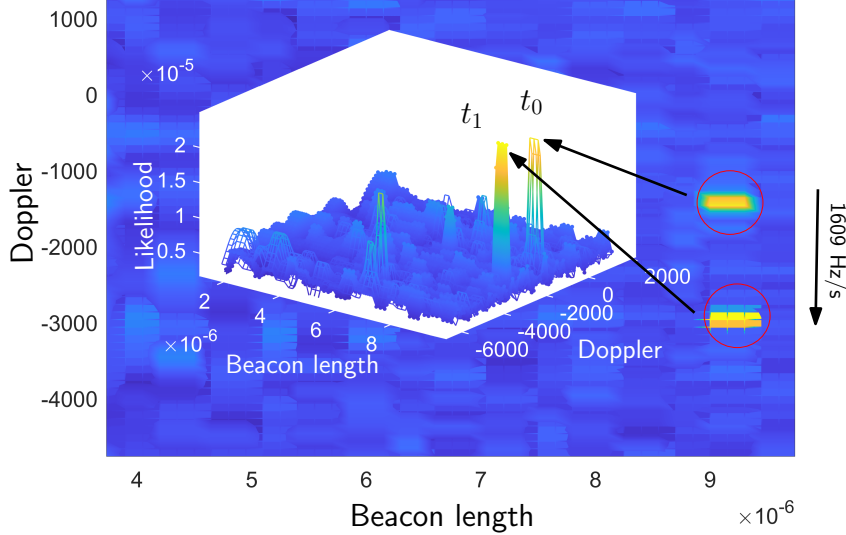


Fig. 2. Matched subspace detection for real Starlink signals: The Doppler-beacon length subspace for two time instances t_0 and t_1 where $t_1 - t_0 = 1s$. In this experiment, the likelihood's location is changed from t_0 to t_1 in the subspace which demonstrates a Doppler rate of 1609 Hz/s for this Starlink LEO SV.

a sufficient number of complete cycles of the beacon signal. As it was mentioned previously, the Doppler frequency $f_D[n]$ cannot be assumed to be constant during the CPI. The signal part of the observation includes a periodic beacon $s[n]$ of length L and its Fourier transform can be written as a pulse train with period $f_0 = \frac{1}{L}$. More precisely,

$$\mathcal{F} \left\{ \sum_{i=-\infty}^{\infty} \alpha \exp(j2\pi f_D[n]n) s[n - iL - n_d] \right\} = \sum_{i=-\infty}^{\infty} \alpha S(i f_0) \Pi(f - f_{D_k} - i f_0), \quad (13)$$

where $S(f) = \mathcal{F}\{s[n]\}$ is the discrete Fourier transform of $s[n]$ and $\Pi(f)$ is the pulse resulting from the time-varying Doppler. As such, a proper sliding band-pass filter, is capable of tracking the Doppler frequency changes in different CPIs from $S(f)$. Tracking the pulse trains from (13) results in an ambiguity of an integer multiple of f_0 in the Doppler estimate. Assuming the Doppler frequency can be modeled as a time polynomial of order p , it can be shown that the peak-tracking estimator will yield an estimation error that is a time polynomial of order $p - 1$. Therefore, the magnitude of the estimation error may grow unacceptably large in a peak-tracking estimator. In many practical scenarios, the instantaneous Doppler frequency can be modeled as a time polynomial during one CPI; therefore, a more sophisticated estimator must be employed. Signals whose frequencies increase or decrease as a time polynomial are referred to as *chirp signals*. A linear chirp can be written as [39]

$$c(t) = \exp(j2\pi(\beta t + \gamma)t), \quad (14)$$

where β and γ are the parameters of the linear chirp signal. In order for the proposed receiver to have a reliable track of the instantaneous Doppler frequency, the chirp parameters have to be taken into account.

A. Wigner Distribution and Chirp Parameter Estimation

One classic way of estimating the parameters of a chirp is through the Wigner distribution [39], which for a single chirp signal $c(t)$ is given by

$$W(t, f) = \int_{-\infty}^{\infty} c\left(t + \frac{\tau}{2}\right) c^*\left(t - \frac{\tau}{2}\right) \exp(-j2\pi f\tau) d\tau. \quad (15)$$

For a linear chirp, i.e., $c(t) = \exp(j2\pi(\beta t^2 + \gamma t))$,

$$W(t, f) = \delta(f - (2\beta t + \gamma)), \quad (16)$$

where $\delta(\cdot)$ is the Dirac delta function. The Wigner distribution concentrates the energy on the time history of the instantaneous frequency and can be used to estimate the parameters of a chirp. Direct implementation of (15) is computationally

inefficient, as the complexity grows with $(ML)^3 \log ML$ [40]. Alternatively, one can search over certain values of Doppler rate, i.e., β_k , wipe-off the effect of β_k in the received signal, and take the FFT of the wiped-off signal to estimate f_{D_k} . This reduces the overall computational complexity of chirp parameter estimation dramatically.

VI. EXPERIMENTAL RESULTS

This section provides the first results for blind Doppler tracking and positioning with Starlink signals of opportunity. A stationary National Instrument (NI) universal software radio peripheral (USRP) 2945R was equipped with a consumer-grade Ku antenna and low-noise block (LNB) downconverter to receive Starlink signals in the Ku band. The sampling rate was set to 2.5 MHz and the carrier frequency was set to 11.325 GHz, which is one of the Starlink downlink frequencies. The samples of the Ku signal were stored for off-line processing.

Next, pseudorange rate observables were formed from the tracked Doppler frequencies by (i) downsampling by a factor D to avoid large time-correlations in the pseudorange observables and (ii) multiplying by the wavelength to express the Doppler frequencies in meters per second.

Let $i \in \{1, 2, 3, 4, 5, 6\}$ denote the SV index. The pseudorange rate observable to the i th SV at time-step $\kappa = k \cdot D$, expressed in meters, is modeled as

$$z_i(\kappa) = \frac{\dot{\mathbf{r}}_{\text{SV}_i}^\top(\kappa) [\mathbf{r}_r - \mathbf{r}_{\text{SV}_i}(\kappa)]}{\|\mathbf{r}_r - \mathbf{r}_{\text{SV}_i}(\kappa)\|_2} + a_i + v_{z_i}(\kappa), \quad (17)$$

where \mathbf{r}_r and $\mathbf{r}_{\text{SV}_i}(\kappa)$ are the receiver's and i th Starlink SV three-dimensional (3-D) position vectors, $\dot{\mathbf{r}}_{\text{SV}_i}(\kappa)$ is the i th Starlink SV 2-D velocity vector, a_i is the constant bias due to the unknown Doppler frequency ambiguity f_0 , and $v_{z_i}(\kappa)$ is the measurement noise, which is modeled as a zero-mean, white Gaussian random variable with variance $\sigma_i^2(\kappa)$. The value of $\sigma_i^2(\kappa)$ is the first diagonal element of $\mathbf{P}_{\kappa|\kappa}$, expressed in m^2/s^2 . Next, define the parameter vector $\mathbf{x} \triangleq [\mathbf{r}_r^\top, a_1, \dots, a_6]^\top$. Let \mathbf{z} denote the vector of all the pseudorange observables stacked together, and let \mathbf{v}_z denote the vector of all measurement noises stacked together, which is a zero-mean Gaussian random vector with a diagonal covariance \mathbf{R} whose diagonal elements are given by $\sigma_i^2(\kappa)$. Then, one can readily write the measurement equation given by $\mathbf{z} = \mathbf{g}(\mathbf{x}) + \mathbf{v}_z$, where $\mathbf{g}(\mathbf{x})$ is a vector-valued function that maps the parameter \mathbf{x} to the pseudorange rate observables according to (17). Next, a weighted nonlinear least-squares (WNLS) estimator with weight matrix \mathbf{R}^{-1} is solved to obtain an estimate of \mathbf{x} given by $\hat{\mathbf{x}} = [\hat{\mathbf{r}}_r^\top, \hat{a}_1, \dots, \hat{a}_6]^\top$. The SV positions were obtained from TLE files and SGP4 software. It is important to note that the TLE epoch time was adjusted for each SV to account for ephemeris errors. This was achieved by minimizing the pseudorange rate residuals for each SV.

Subsequently, the receiver position was estimated using the aforementioned WNLS. The 3-D position error was found to be 22.9 m, while the 2-D position error was 10 m.

A skyplot of the Starlink SVs as well as the environment layout along with the positioning results are shown in Fig. 3.

VII. CONCLUSION

The first Doppler positioning-based results with Starlink LEO SVs was demonstrated. In order to detect Starlink's LEO SV signals and track the Doppler frequencies of each Starlink LEO SV, a cognitive opportunistic framework was used. To this end, a GLR-based test was developed to detect the LEO SV signals and estimate their corresponding beacons. A chirp parameter estimator was also proposed to track the Doppler frequencies from the unknown Starlink signals. Experimental results showed a horizontal positioning error of 10 m by tracking the Doppler of six Starlink LEO SVs.

ACKNOWLEDGMENTS

This work was supported in part by the Office of Naval Research (ONR) under Grant N00014-19-1-2511, in part by the U.S. Department of Transportation (USDOT) under Grant 69A3552047138 for the CARMEN University Transportation Center (UTC), and in part by the National Science Foundation (NSF) under Grant 1929965.

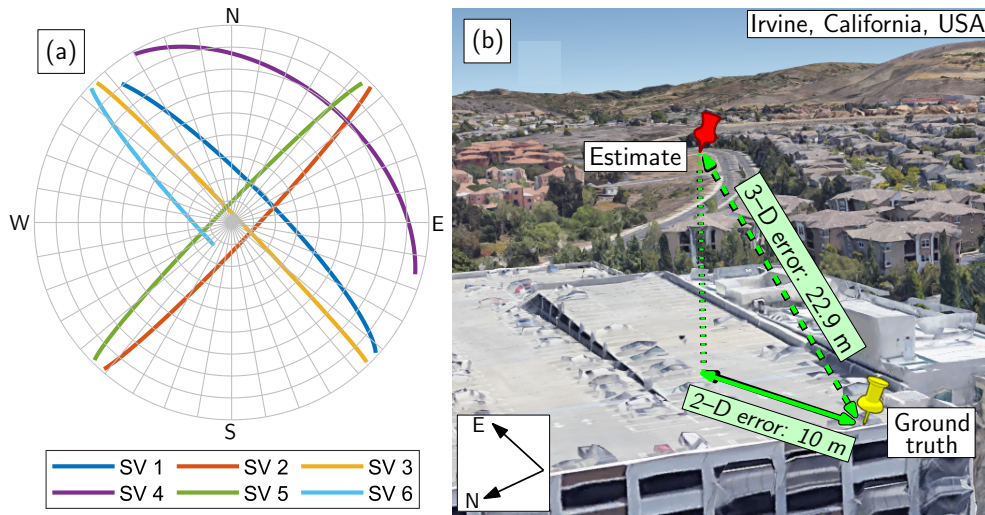


Fig. 3. (a) Skyplot showing the Starlink SVs' trajectories during the experiment. (b) Environment layout and positioning results.

References

- [1] M. Rabinowitz, B. Parkinson, C. Cohen, M. O'Connor, and D. Lawrence, "A system using LEO telecommunication satellites for rapid acquisition of integer cycle ambiguities," in *Proceedings of IEEE/ION Position Location and Navigation Symposium*, April 1998, pp. 137–145.
- [2] N. Levanon, "Quick position determination using 1 or 2 LEO satellites," *IEEE Transactions on Aerospace and Electronic Systems*, vol. 34, no. 3, pp. 736–754, July 1998.
- [3] M. Joerger, L. Gratton, B. Pervan, and C. Cohen, "Analysis of Iridium-augmented GPS for floating carrier phase positioning," *NAVIGATION, Journal of the Institute of Navigation*, vol. 57, no. 2, pp. 137–160, 2010.
- [4] T. Reid, A. Neish, T. Walter, and P. Enge, "Broadband LEO constellations for navigation," *NAVIGATION, Journal of the Institute of Navigation*, vol. 65, no. 2, pp. 205–220, 2018.
- [5] D. Racelis, B. Pervan, and M. Joerger, "Fault-free integrity analysis of mega-constellation-augmented GNSS," in *Proceedings of ION GNSS Conference*, January 2019, pp. 465–484.
- [6] P. Iannucci and T. Humphreys, "Economical fused LEO GNSS," in *Proceedings of IEEE/ION Position, Location and Navigation Symposium*, 2020, pp. 426–443.
- [7] J. Khalife, M. Neinavaie, and Z. Kassas, "Navigation with differential carrier phase measurements from megaconstellation LEO satellites," in *Proceedings of IEEE/ION Position, Location, and Navigation Symposium*, April 2020, pp. 1393–1404.
- [8] Z. Kassas, J. Khalife, M. Neinavaie, and T. Mortlock, "Opportunity comes knocking: overcoming GPS vulnerabilities with other satellites' signals," *Inside Unmanned Systems Magazine*, pp. 30–35, June/July 2020.
- [9] R. Morales-Ferre, E. Lohan, G. Falco, and E. Falletti, "GDOP-based analysis of suitability of LEO constellations for future satellite-based positioning," in *Proceedings of IEEE International Conference on Wireless for Space and Extreme Environments*, 2020, pp. 147–152.
- [10] Z. Kassas, "Position, navigation, and timing technologies in the 21st century," J. Morton, F. van Diggelen, J. Spilker, Jr., and B. Parkinson, Eds. Wiley-IEEE, 2021, vol. 2, ch. 43: Navigation from low Earth orbit – Part 2: models, implementation, and performance, pp. 1381–1412.
- [11] T. Reid, T. Walter, P. Enge, D. Lawrence, H. Cobb, G. Gutt, M. O'Conner, and D. Whelan, "Position, navigation, and timing technologies in the 21st century," J. Morton, F. van Diggelen, J. Spilker, Jr., and B. Parkinson, Eds. Wiley-IEEE, 2021, vol. 2, ch. 43: Navigation from low Earth orbit – Part 1: Concept, Current Capability, and Future Promise, pp. 1359–1379.
- [12] S. Thompson, S. Martin, and D. Bevely, "Single differenced doppler positioning with low Earth orbit signals of opportunity and angle of arrival estimation," in *Proceedings of ION International Technical Meeting*, 2020, pp. 497–509.
- [13] N. Khairallah and Z. Kassas, "Ephemeris closed-loop tracking of LEO satellites with pseudorange and Doppler measurements," in *Proceedings of ION GNSS Conference*, September 2021, accepted.
- [14] S. Kozhaya, J. Haidar-Ahmad, A. Abdallah, S. Saab, and Z. Kassas, "Comparison of neural network architectures for simultaneous tracking and navigation with LEO satellites," in *Proceedings of ION GNSS Conference*, September 2021, accepted.
- [15] T. Reid, K. Gunning, A. Perkins, S. Lo, and T. Walter, "Going back for the future: Large/mega LEO constellations for navigation," in *Proceedings of ION GNSS Conference*, September 2019, pp. 2452–2468.
- [16] T. Reid, B. Chan, A. Goel, K. Gunning, B. Manning, J. Martin, A. Neish, A. Perkins, and P. Tarantino, "Satellite navigation for the age of autonomy," in *Proceedings of IEEE/ION Position, Location and Navigation Symposium*, 2020, pp. 342–352.
- [17] A. Nardin, F. Doyis, and J. Fraire, "Empowering the tracking performance of LEO-based positioning by means of meta-signals," *IEEE Journal of Radio Frequency Identification*, pp. 1–1, 2021.
- [18] Z. Kassas, J. Morales, and J. Khalife, "New-age satellite-based navigation – STAN: simultaneous tracking and navigation with LEO satellite signals," *Inside GNSS Magazine*, vol. 14, no. 4, pp. 56–65, 2019.
- [19] J. Khalife, M. Neinavaie, and Z. Kassas, "The first carrier phase tracking and positioning results with Starlink LEO satellite signals," *IEEE Transactions on Aerospace and Electronic Systems*, 2021, accepted.
- [20] L. Scharf and B. Friedlander, "Matched subspace detectors," *IEEE Transactions on signal processing*, vol. 42, no. 8, pp. 2146–2157, 1994.
- [21] S. Kraut, L. Scharf, and L. McWhorter, "Adaptive subspace detectors," *IEEE Transactions on Signal Processing*, vol. 49, no. 1, pp. 1–16, 2001.
- [22] F. Gini and A. Farina, "Vector subspace detection in compound-Gaussian clutter. part I: survey and new results," *IEEE Transactions on Aerospace and Electronic Systems*, vol. 38, no. 4, pp. 1295–1311, 2002.
- [23] M. Korso, R. Boyer, A. Renaux, and S. Marcos, "Statistical resolution limit for source localization with clutter interference in a MIMO radar context," *IEEE Transactions on Signal Processing*, vol. 60, no. 2, pp. 987–992, 2012.

- [24] A. Zaimbashi, M. Derakhtian, and A. Sheikhi, "GLRT-based CFAR detection in passive bistatic radar," *IEEE Transactions on Aerospace and Electronic Systems*, vol. 49, no. 1, pp. 134–159, 2013.
- [25] I. Atitallah, A. Kammoun, M. Alouini, and T. Al-Naffouri, "Optimal design of large dimensional adaptive subspace detectors," *IEEE Transactions on Signal Processing*, vol. 64, no. 19, pp. 4922–4935, 2016.
- [26] A. Comberoux, F. Pascal, and G. Ginolhac, "Performance of the low-rank adaptive normalized matched filter test under a large dimension regime," *IEEE Transactions on Aerospace and Electronic Systems*, vol. 55, no. 1, pp. 459–468, 2019.
- [27] M. Wax and A. Adler, "Detection of the number of signals by signal subspace matching," *IEEE Transactions on Signal Processing*, vol. 69, pp. 973–985, 2021.
- [28] Z. Wang, G. Li, and H. Chen, "Adaptive persymmetric subspace detectors in the partially homogeneous environment," *IEEE Transactions on Signal Processing*, vol. 68, pp. 5178–5187, 2020.
- [29] D. Ciunzo, A. De Maio, and D. Orlando, "On the statistical invariance for adaptive radar detection in partially homogeneous disturbance plus structured interference," *IEEE Transactions on Signal Processing*, vol. 65, no. 5, pp. 1222–1234, 2017.
- [30] G. Gao, "Towards navigation based on 120 satellites: Analyzing the new signals," Ph.D. dissertation, Stanford University, 2008.
- [31] J. Merwe, S. Bartl, C. O'Driscoll, A. Rügamer, F. Förster, P. Berglez, A. Popugaev, and W. Felber, "GNSS sequence extraction and reuse for navigation," in *Proceedings of ION GNSS+ Conference*, 2020, pp. 2731–2747.
- [32] M. Neinavaie, J. Khalife, and Z. Kassas, "Blind Doppler tracking and beacon detection for opportunistic navigation with LEO satellite signals," in *Proceedings of IEEE Aerospace Conference*, March 2021, pp. 1–8.
- [33] J. Khalife, M. Neinavaie, and Z. Kassas, "Blind Doppler tracking from OFDM signals transmitted by broadband LEO satellites," in *Proceedings of IEEE Vehicular Technology Conference*, April 2021, pp. 1–6.
- [34] M. Neinavaie, J. Khalife, and Z. Kassas, "Cognitive opportunistic navigation in private networks with 5G signals and beyond," *IEEE Journal of Selected Topics in Signal Processing*, 2021, accepted.
- [35] I. Del Portillo, B. Cameron, and E. Crawley, "A technical comparison of three low earth orbit satellite constellation systems to provide global broadband," *Acta Astronautica*, vol. 159, pp. 123–135, 2019.
- [36] K. Shamaei and Z. Kassas, "Receiver design and time of arrival estimation for opportunistic localization with 5G signals," *IEEE Transactions on Wireless Communications*, vol. 20, no. 7, pp. 4716–4731, 2021.
- [37] D. Tse and P. Viswanath, *Fundamentals of wireless communication*. Cambridge university press, 2005.
- [38] S. Kay, *Fundamentals of statistical signal processing: Detection Theory*. Prentice-Hall, Upper Saddle River, NJ, 1993, vol. II.
- [39] P. Djuric and S. Kay, "Parameter estimation of chirp signals," *IEEE Transactions on Acoustics, Speech, and Signal Processing*, vol. 38, no. 12, pp. 2118–2126, 1990.
- [40] M. Vishwanath, R. Owens, and M. Irwin, "The computational complexity of time-frequency distributions," in *Proceedings of IEEE Workshop on Statistical Signal and Array Processing*, 1992, pp. 444–447.